Electronic Materials Letters, Vol. 5, No. 2 (2009), pp. 77-81
DOI: 10.3365/eml.2009.06.077

Mechanical Synthesis and Rapid Consolidation of a Nanocrystalline Cu-Al_2O_3 Composite by High Frequency Induction Heated Sintering

In-Jin Shon,[1,2,*] Jin-Yeoung Lee,[1] Kee-Seok Nam,[3] Byung-Moon Moon,[4] and Dong-Mok Lee[1]

[1]Division of Advanced Materials Engineering and the Research Center of Advanced Materials Development, Engineering College, Chonbuk National University, 664-14 Deokjin-dong, Deokjin-gu, Jeonju-si, Jeonbuk 561-756, Korea
[2]Department of Hydrogen and Fuel Cells Engineering, Specialized Graduate School, Chonbuk National University, Jeonbuk 561-756, Korea
[3]Korea Institute of Materials Science 531 Changwondaero, Changwon-si, Gyeongnam 641-831, Korea
[4]Liquid Processing & Casting Technology R&D Department, Korea Institute of Industrial Technology, 7-47 Songdo-dong, Yeonsu-gu, Incheon 406-840, Korea

Cu and Al_2O_3 nanopowders were synthesized from 3CuO and 2Al by high energy ball milling. The powder sizes of Cu and Al_2O_3 were 14 nm and 133 nm, respectively. A dense nanocrystalline 3Cu-Al_2O_3 composite was consolidated by a high frequency induction heated sintering method within 2 minutes from the mechanically synthesized powders. The average hardness and fracture toughness values of the nanostuctured 3Cu-Al_2O_3 composite were 520 kg/mm^2 and 5 MPa·m$^{1/2}$, respectively.

Keywords: high frequency induction heated sintering, composite, nanomaterial, mechanical properties, Cu-Al_2O_3

1. INTRODUCTION

While copper is widely used in industry its principal limitation is low hardness, especially when employed in electrical contact applications. The attractive physical and mechanical properties that can be obtained with metal matrix composites, including high specific modulus, strength-to weigh ratio, fatigue strength, temperature stability, and wear resistance, have been extensively documented.[1-5]

Traditionally, discontinuously reinforced metal matrix composites have been produced by several processing routes such as powder metallurgy, spray deposition mechanical alloying, various casting techniques, and SHS (self-propagating high temperature synthesis). These techniques are based on the addition of ceramic reinforcements to the matrix materials, which may be in molten or powder form. Among these techniques, high energy ball milling and mechanical alloying of powder mixtures, which involve mechanical milling and chemical reactions, have been reported to be efficient methods for the preparation of nano-crystalline metals and alloys.[6]

Offering broad functional diversity and exhibiting enhanced or different properties compared with bulk materials, nanostructured materials have been widely investigated [7,8]. In the case of nanostructured ceramics in particular, the presence of a large fraction of grain boundaries can lead to unusual or superior mechanical, electrical, optical, sensing, magnetic, and biomedical properties.[9-15] Nanocrystalline powders have recently been developed by co-precipitation, a thermochemical and thermomechanical process referred to as a spray conversion process (SCP), and high energy milling.[16,17] The grain size in sintered materials, however, becomes much larger than that in pre-sintered powders due to rapid grain growth during the conventional sintering process. Although the initial particle size is less than 100 nm, the grain size increases rapidly up to 500 nm or larger during conventional sintering.[18] As such, control of grain growth during sintering is one of the keys to the commercial success of nanostructured materials. In this regard, the high frequency induction activated sintering method, whereby dense materials can be produced within 2 min, has been shown to be effective in achieving this goal.[19]

The purpose of the present work is to produce nanopowders of Cu, Al_2O_3, and a dense nanocrystalline Cu-Al_2O_3 composite within 2 minutes from mechanically synthesized powders by using this novel induced current activated sintering method and to evaluate the mechanical properties (hardness and fracture toughness) of the produced powders.

2. EXPERIMENTAL PROCEDURE

Powders of 99% CuO (< 5 μm, Aldrich, Inc) and 99%

*Corresponding author: ijshon@chonbuk.ac.kr

pure Al (-325 mesh, Cerac, Inc) were used as starting materials. 3CuO and 2Al powder mixtures were first milled in a Pulverisette-5 planetary mill, a high-energy ball mill, at 250 rpm and for 10 hrs. Tungsten carbide balls (8.5 mm in diameter) were used in a sealed cylindrical stainless steel vial under an argon atmosphere. The weight ratio of the ball-to-powder was 30:1. Milling resulted in a significant reduction of grain size. The grain sizes of Cu and Al_2O_3 were calculated by C. Suryanarayana and M. Grant Norton's formula,[20]

$$B_r\,(B_{crystalline}+B_{strain})\cos\theta = k\,\lambda / L + \eta\sin\theta \quad (1)$$

where B_r is the full width at half-maximum (FWHM) of the diffraction peak after instrument correction; $B_{crystalline}$ and B_{strain} are FWHM caused by small grain size and internal stress, respectively; k is a constant (with a value of 0.9); λ is the wavelength of the X-ray radiation; L and η are grain size and internal strain, respectively; and θ is the Bragg angle. The parameters B and B_r follow Cauchy's form with the relationship $B = B_r + B_s$, where B and B_s are the FWHM of the broadened Bragg peaks and the standard sample's Bragg peaks, respectively.

After milling, the mixed powders were placed in a graphite die (outside diameter, 45 mm; inside diameter, 20 mm; height, 40 mm) and then introduced into the high frequency induction heated sintering system made by Eltek in South Korea, shown schematically in Fig. 1. The four major stages in the synthesis are as follows. The system was evacuated (stage 1). A uniaxial pressure of 80 MPa was then applied (stage 2). A pulsed current was then activated and maintained until densification was attained, as indicated by measurement of the shrinkage of the sample via a linear gauge (stage 3). Temperature was measured by a pyrometer on the surface of the graphite die. At the end of the process, the sample was cooled to room temperature (stage 4).

The relative densities of the synthesized sample were measured by the Archimedes method. Microstructural information was obtained from polished product samples. Compositional and microstructural analyses of the products were made through X-ray diffraction (XRD) and scanning electron microscopy (SEM) with an energy dispersive X-ray analysis (EDAX). Vickers hardness was measured by performing indentations on the synthesized samples under a load of 20 kg and a dwell time of 15 s.

3. RESULTS AND DISCUSSION

The interaction between 3CuO and 2 Al, i.e.,

$$3CuO + 2\,Al \rightarrow 3Cu + Al_2O_3, \quad (2)$$

is thermodynamically feasible, as shown in Fig. 2.

The X-ray diffraction pattern of mechanically milled powders from raw powders is shown in Fig. 3(c). Reactant phase peaks are not detected but product phase (Al_2O_3, Cu) peaks are observed. From the above results, it is determined that a solid replacement reaction completely occurs. The full width at half-maximum (FWHM) of the diffraction peak is broad due to refinement of the powder and strain. The average grain sizes of Al_2O_3 and Cu measured according to C. Suryanarayana and M. Grant Norton's formula were about 14 nm and 133 nm, respectively.

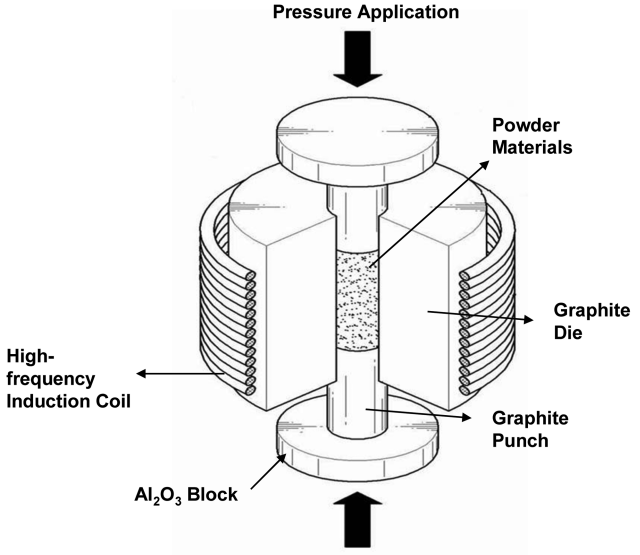

Fig. 1. Schematic diagram of the high frequency induction heated sintering apparatus.

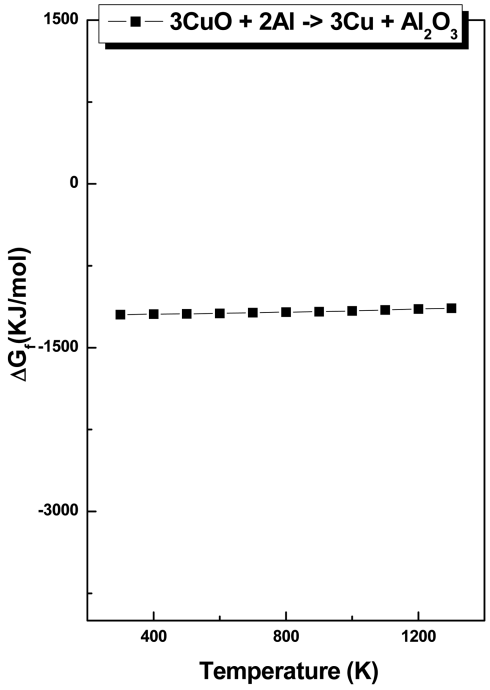

Fig. 2. Temperature dependence of the Gibbs free energy variation by interaction of 3CuO with 2Al.

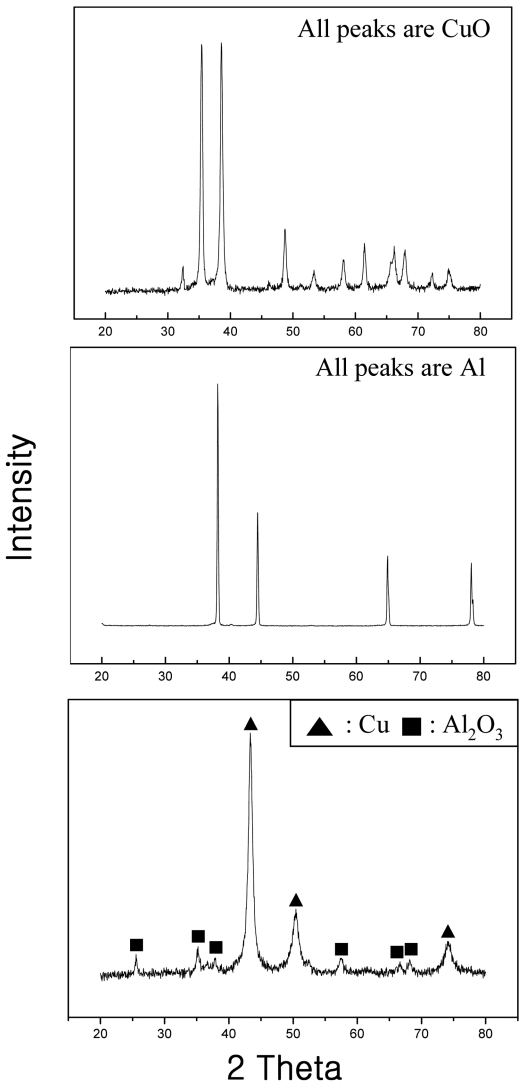

Fig. 3. XRD patterns of raw materials and mechanically synthesized powder: (a) CuO, (b) Al and (c) mechanically milled 2Al + 3CuO.

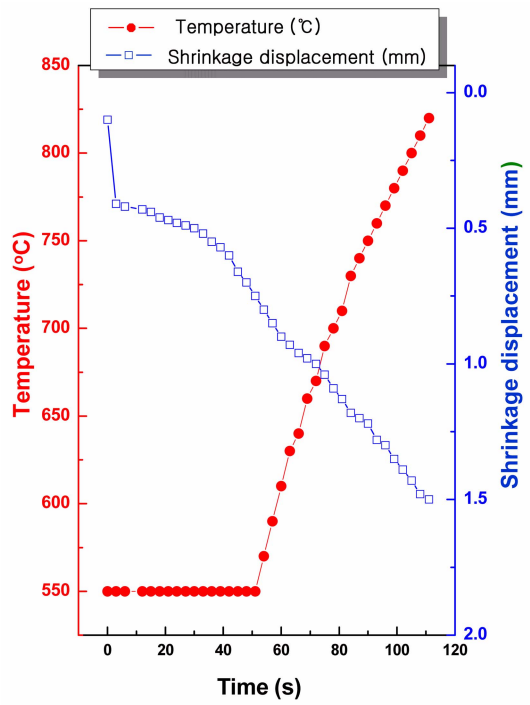

Fig. 4. Variations of temperature and shrinkage displacement with heating time during high frequency induction heated sintering of the 3Cu-Al_2O_3 composite.

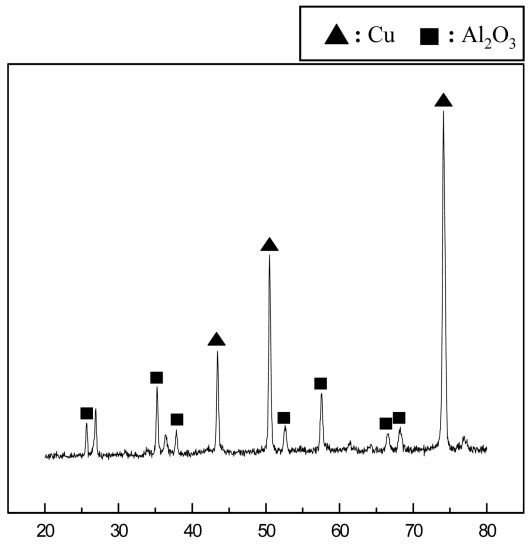

Fig. 5. XRD pattern of the Cu-Al_2O_3 composite heated to 820.

The variations in shrinkage displacement and temperature of the surface of the graphite die with heating time during the processing of Al_2O_3 and 3Cu system are shown Fig. 4. As the induced current is applied, the shrinkage displacement continuously increased up to about 820°C. The XRD pattern of the Cu-Al_2O_3 composite heated to 820 is shown in Fig. 5. The average grain sizes of Cu and Al_2O_3—constituting the structural parameters in this study—obtained from X-ray data in Fig. 5 using C. Suryanarayana and M. Grant Norton's formula are 87 nm and 256 nm, respectively. Thus, the average grain size of the sintered Cu-Al_2O_3 is roughly the same as that of the initial powder, indicating the absence of grain growth during sintering. This retention of grain size is attributed to the high heating rates and the relatively short high temperature exposure of the powders. Figure 6 shows a BSE (back scattered electron) image of mechanically milled powders and a specimen heated to 820, respectively. The Al_2O_3 and Cr particles are well distributed in the matrix, as ascertained by the BSE image shown in Fig. 6(b).

Vickers hardness measurements were performed on polished sections of the Cu-Al_2O_3 composite using a 20 kg_f load and 15 s dwell time. The calculated hardness value of the Cu-Al_2O_3 composite was 520 kg/mm^2. This value represents an average of five measurements. Indentations with suffi-

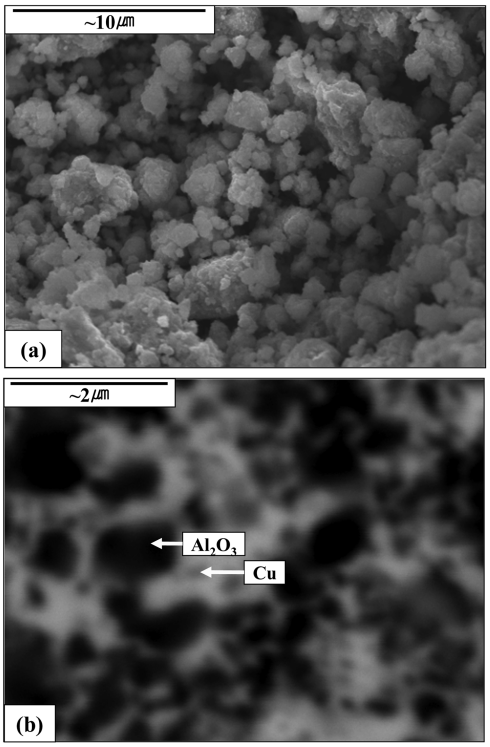

Fig. 6. Back scattered electron images of the 3Cu-Al_2O_3 system: (a) after high energy ball milling, (b) after sintering.

ciently large loads produced median cracks around the indent. From the length of these cracks, the fracture toughness values can be determined using the following formula reported by Anstis *et al*.[21]:

$$K_{IC} = 0.016\,(E/H)^{1/2} \cdot P/C^{3/2} \quad (3)$$

where E is Young's modulus, H the indentation hardness, P the indentation load, and C the trace length of the crack measured from the center of the indentation. The modulus was estimated by the rule mixtures for a 0.547 volume fraction of Al_2O_3 and a 0.453 volume fraction of Cu using E(Al_2O_3) = 380 GPa[22] and E(Cu) = 130 Gpa.[23] As in the case of the hardness values, the toughness values were derived from the average of five measurements. The toughness values obtained by the aforementioned two methods of calculation are 5 MPa·$m^{1/2}$.

A typical indentation pattern for the Cu-Al_2O_3 composite is shown in Fig. 7. Typically, one to three additional cracks propagating from the indentation corner were observed. This shows the the cracks propagate linearly. The hardness and fracture toughness of Al_2O_3 with a grain size of 4.5 μm are reported as 1800 kg/mm^2 and 4 MPa·$m^{1/2}$, respectively [22]. The hardness of the 3Cu-Al_2O_3 composite is lower than that of monolithic Al_2O_3 but the fracture toughness is higher than that of Al_2O_3 due to the addition of ductile Cu. A higher magnification view of the indentation median crack in the composite is presented in Fig. 7(b), showing that the crack propagates reflectively.

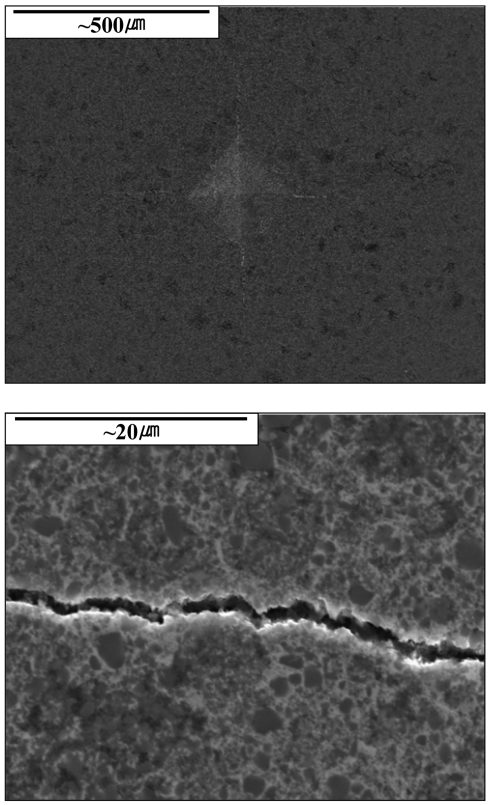

Fig. 7. (a) Vickers hardness indentation and (b) median crack propagating of the Cu-Al_2O_3 composite.

4. CONCLUSIONS

Nanopowders of Al_2O_3 and Cu were synthesized from 2Al and 3CuO by high energy ball milling. The powder sizes of Cu and Al_2O_3 were 14nm and 133nm, respectively. Using the high frequency induction heated sintering method, densification of a nanostructured 3Cu-Al_2O_3 composite was accomplished from mechanically synthesized powders within a duration of 2 min. The average grain sizes of Cu and Al_2O_3 prepared by HFIHS were about 87 nm and 256 nm, respectively. The average hardness and fracture toughness values obtained were 520 kg/mm^2 and 5 MPa·$m^{1/2}$, respectively. The fracture toughness of the 3Cu-Al_2O_3 composite is higher than that of monolithic Al_2O_3 with a grain size of 4.5 μm.

ACKNOWLEDGMENT

This research was supported by the Basic Research Project of the Korea Institute of Geoscience and Mineral Resources (KIGAM).

REFERENCES

1. L. Ceschini, G. Minak, and A. Morri, *Compos. Sci. Technol.* **66**, 333 (2006).
2. S. C. Tjong and Z. Y. Ma, *Mater. Sci. Eng.* **29**, 49 (2000).
3. D. J. Lloyd, *Int. Mater. Rev.* **39**, 1 (1994).
4. J. M. Torralba and F. Velasco, *J. Mater. Process. Technol.* **133**, 203 (2003).
5. R. Fan, B. Liu, J. Zhang, J. Bi, and Y. Yin, *Mater. Chem. Phys*. **91**, 40 (2005).
6. S. Paris, E. Gaffet, F. Bernard, and Z.A. Munir, *Scripta Mater.* **50**, 691 (2004).
7. H. Gleiter, *Nanostruct. Mater.* **6**, 3 (1995).
8. J. R. Yoon, D. J. Choi, K. H. Lee, J. Y. Lee, and Y. H. Kim, *Electron. Mater. Lett.* **4**, 167 (2008)
9. J. Karch, R. Birringer, and H. Gleiter, *Nature.* **330**, 556 (1987).
10. A. M. George, J. Iniguez, and L. Bellaiche, *Nature.* **413**, 54 (2001).
11. D. Hreniak and W. Strek, *J. Alloy. Compd.* **341**, 183 (2002).
12. C. Xu, J. Tamaki, N. Miura, and N. Yamazoe, *Sensor. Actuat. B: Chem.* **3**, 147 (1991).
13. D. G. Lamas, A. Caneiro, D. Niebieskikwiat, R. D. Sanchez. D. Garcia, and B. Alascio, *J. Magn. Magn. Mater.* **241**, 207 (2002).
14. C. Nahm, C. Kim, Y. Park, B. Lee, and B. Park, *Electron. Mater. Lett.* **4**, 5 (2008).
15. E. S. Ahn, N. J. Gleason, A. Nakahira, and J. Y. Ying, *Nano Lett.* **1**, 149 (2001).
16. Z. Fang, and J.W. Eason, *Int. J. Refract. Met. Hard Mater.* **13**, 297 (1995).
17. A. I. Y. Tok, L. H. Luo, and F. Y. C. Boey, *Mater. Sci. Eng. A.* **383**, 229 (2004).
18. M. Sommer, W. D. Schubert, E. Zobetz, and P. Warbichler, *Int. J. Refract. Met. Hard Mater.* **20**, 41 (2002).
19. H. C. Kim, I. J. Shon, I. K. Jeong, I. Y. Ko, J. K. Yoon, and J. M. Doh, *Met. Mater. Int.* **13**, 39 (2007).
20. C. Suryanarayana, and M. Grant Norton, *X-ray Diffraction A Practical Approach*, p. 213, Plenum Press, New York (1998).
21. G. R. Anstis, P. Chantikul, B. R. Lawn, and D. B. Marshall, *J. Am. Ceram. Soc.* **64**, 533 (1981).
22. M. N. Rahaman, A. Yao, B. S. Bal, J. P. Garino, and M. D. Ries, *J. Am. Ceram. Soc.* **90**, 1965 (2007).
23. http://en.wikipedia.org/wiki/Elastic properties of the elements (data page).